Enhanced thermal transport across multilayer graphene and water by interlayer functionalization

Bing-Yang Cao,[1,a)] Ji-Hang Zou,[1] Guo-Jie Hu,[2] and Gui-Xing Cao[2]
[1]*Key Laboratory for Thermal Science and Power Engineering of Ministry of Education, Department of Engineering Mechanics, Tsinghua University, Beijing 100084, China*
[2]*Institute of Telecommunication Satellite, China Academy of Space Technology, Beijing 100094, China*

(Received 8 December 2017; accepted 13 January 2018; published online 25 January 2018)

Graphene has attracted enormous attention due to its extraordinary physical properties, which have potential for increasing the thermal conductivity of nanocomposites or nanofluids, and the thermal resistance between graphene and the surrounding matrices arises as an important issue. In this paper, the thermal transport at the graphene-water interface is investigated by molecular dynamics simulations. The interfacial thermal resistance decreases with the graphene layer number. Interlayer functionalization by oxygen atoms is applied to tune the interfacial thermal resistance. A peak thermal resistance reduction of nearly 50% is generated with the oxygen ratio of only 0.5% for two-layer graphene. Based on the analyses of vibrational density of states, it is found that lower thermal resistance is consistent with more vibrational density of states overlaps at the interface. Our results are instructive for improving the interfacial thermal transport in graphene-based nanocomposites and nanofluids. *Published by AIP Publishing.* https://doi.org/10.1063/1.5018749

The superior thermal conductivity of graphene, 3000–5000 W/(m K) at room temperature[1–3] owing to the long mean free path of flexural acoustic phonons,[4–8] has inspired massive interest in the thermal management fields of electronic and optic devices.[9] One promising application of graphene flakes is as fillers to enhance the thermal properties of organic materials or nanofluids.[10–16] Literature has confirmed that graphene-based polymers exhibit excellent thermal performance and have potential to be used as thermal interface materials.[10] Veca *et al.*[11] reported an extremely high thermal conductivity of about 80 W/(m K) for the epoxy composites by adding 33 vol. % graphene nanosheets. Shahil and Balandin[12] found that the graphene/epoxy composite exhibits a significant increase of thermal conductivity by 2300% at the filler loading fraction of only 10 vol. % using the laser flashing measurements. Graphene is also a good candidate for improving the heat conduction in nanofluids, which may perform better than carbon nanotubes (CNTs) due to its high intrinsic thermal conductivity.[13] It was revealed that the thermal conductivity of deionized water shows an enhancement by 14% at 298 K with a very low graphene concentration of 0.056 vol. %.[14] On the basis of the transient hot wire method, Ref. 15 uncovered that the thermal conductivity of nanofluids is 27% higher than that of pure water with 0.2 vol. % concentration of graphene fillers at 323 K.

However, the thermal conductivities of graphene-based composites are far below the theoretically expected values despite the remarkable thermal properties of graphene. One main reason is that low thermal conductance at the graphene-matrix interface strongly limits the thermal transport in the composites.[12,17–20] Chemical functionalization, which might strengthen the interfacial bonding and facilitate the phonon vibrational coupling, is an effective route to reduce the thermal resistance at the interfaces.[18–25] Konatham and Striolo[18] discovered that the thermal resistance at the graphene-oil interface could be largely reduced by functionalizing graphene with alkanes based on molecular dynamics (MD) simulations. Alexeev *et al.*[26] found that the thermal resistance at the graphene-water interface depends on the density of the adjacent water layer and can be tuned by cross-plane pressure and graphene hydrophobicity. Although many efforts have been devoted to the research of thermal transport in graphene-based composites, little focus is put on the role of interlayer coupling in multilayer graphene (MLG). Since MLG is widely used in engineering applications,[10,12] it is of great significance to investigate the interfacial thermal transport at the MLG-matrix interface.

In the current work, MD simulations are performed to study the thermal transport across graphene and water with the LAMMPS package.[27] Single-layer graphene (SLG) and MLG (layer number n = 2–5) in water are constructed and simulated. As seen in Fig. 1(a), two-layer graphene is sandwiched between two water layers as one case. The in-plane size of graphene is about 10 nm × 10 nm, and the interlayer distance is 0.335 nm. Each water layer has the size of 10 nm × 10 nm × 5 nm. The optimized Tersoff potential,[28,29] which may accurately display the phonon dispersion of graphene, is adopted to describe the C-C covalent interactions.[29,30] The extended simple point charge (SPC/E) model[31] is used to represent the interactions between water molecules. Carbon-water bonding and the interlayer coupling in MLG are van der Waals type, modeled by the Lennard-Jones (LJ) function $V(r_{ij}) = 4\epsilon\left[\left(\frac{\sigma}{r_{ij}}\right)^{12} - \left(\frac{\sigma}{r_{ij}}\right)^{6}\right]$ with the parameters taken from Refs. 32 and 33, respectively. Periodic boundary conditions are employed for all directions. The thermal relaxation simulations mimicking the pump-probe experimental method[34,35] are performed to obtain the interfacial thermal resistance. The time step is set as 0.5 fs. The simulation

a)Author to whom correspondence should be addressed: caoby@tsinghua.edu.cn. Tel./Fax: +86-10-6279-4531.

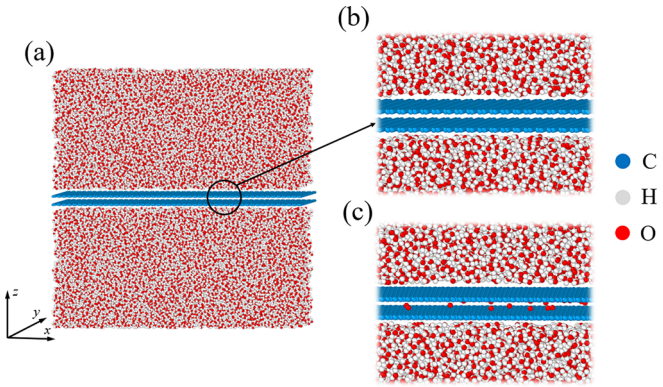

FIG. 1. (a) Simulation system of two-layer graphene embedded in water in the initial state. (b) The zoomed in view of (a). (c) The zoomed in view of two-layer graphene functionalized by interlayer oxygen atoms in water.[37]

procedure starts with the NPT ensemble (constant mass, pressure, and temperature) at the temperature of 300 K and the cross-plane pressure of 1 atm for 100 ps. Then, another 100 ps is operated to equilibrate the system at 300 K with a constant volume. Afterward, the temperature of graphene is instantaneously increased to 500 K, while the temperature of water remains at 300 K using separate Nosé-Hoover thermostats for 10 ps.[36] At last, the entire system is allowed to relax under the NVE ensemble (constant mass, volume, and energy) with the thermostats removed. In the thermal relaxation process, the relaxation time τ could be extracted from the exponential relation $\Delta T(t) = \Delta T(0)\exp\left(-\frac{t}{\tau}\right)$, where $\Delta T(t)$ is the temperature difference between graphene and water decaying with the time t (see supplementary material for details). Given that the thermal resistance of the interface is much higher than that of graphene, the interfacial thermal resistance R is derived from the lumped heat-capacity model as[21]

$$R = \frac{\tau A}{C_V}, \tag{1}$$

where A is the contact area and C_V is the heat capacity of graphene.

It is validated that the graphene domain size and the initial temperature difference have negligible effects on the calculated interfacial thermal resistance (presented in the supplementary material). As plotted in Fig. 2, the thermal resistance at the graphene-water interface decreases with the graphene layer number. The SLG-water interfacial thermal resistance is $6.70\pm0.32\times10^{-8}$ m^2 K/W, which agrees well with that of the CNT-surfactant-water interface derived from transient absorption measurements.[34] Compared to SLG, two-layer graphene may couple better with water as the interfacial thermal resistance is reduced by ~40%. With the increasing layer number for MLG, the thermal resistance shows a slight decline at the graphene-water interface. A similar size dependence at the MLG-water interface was uncovered by Ref. 26, owing to the large phonon mean free path in the out-of-plane axis of MLG. Hu *et al.*[38] studied the thermal transport across MLG and phenolic resin and also found that the interfacial thermal resistance decreases with increasing graphene layers.

To elucidate the root of the layer dependent thermal resistance, the vibrational density of states (VDOS) is obtained for

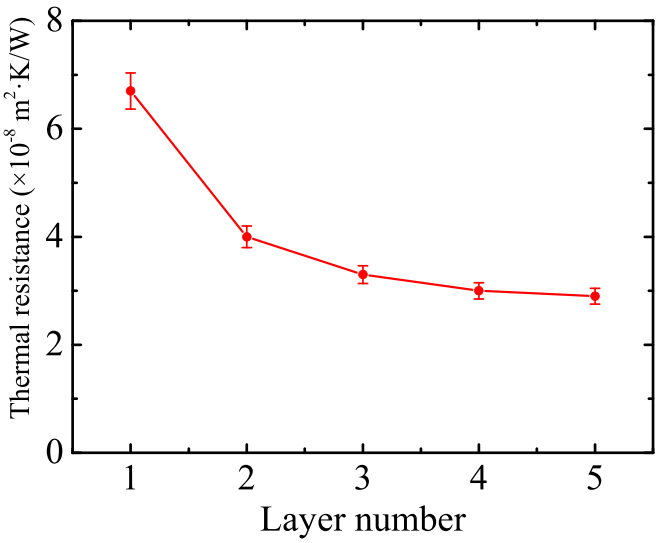

FIG. 2. Interfacial thermal resistance between graphene and water varying with the graphene layer number.

graphene and water from the Fourier transform of the velocity autocorrelation

$$D(\omega) = \int_0^{\tau_0} \frac{\langle v(0)\cdot v(t)\rangle}{\langle v(0)\cdot v(0)\rangle}\exp(-2\pi i\omega t)dt. \tag{2}$$

Here, $D(\omega)$ is the VDOS at the frequency ω in the heat transfer process, τ_0 is the integration time, and $\langle v(0)\cdot v(t)\rangle$ is the velocity autocorrelation function. As shown in Fig. 3, the dominant vibrations are high-frequency modes in SLG, while major modes are low-frequency vibrations in water. The massive mismatch of VDOS might be one of the critical reasons for the high thermal resistance between SLG and water because a small overlap of VDOS implies that heat flow may not go across the interface easily.[39,40] As to two-layer graphene, high-frequency modes are much suppressed, especially for those around the density peak of 49 THz. Besides, a new VDOS peak of 2.4 THz appears in two-layer graphene and is close to the water VDOS peak of 2.0 THz. When the layer number increases to five, the VDOS at the interface has negligible changes except for higher values around the peak 2.4 THz compared to two-layer graphene.

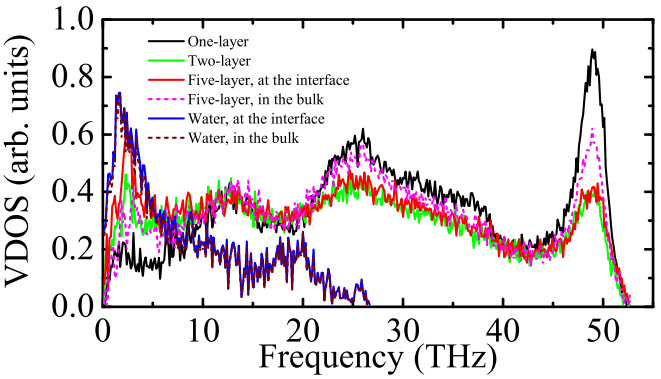

FIG. 3. Vibrational density of states for graphene and water. Graphene at the interface is the outermost layer, while graphene in the bulk is the middle part of five-layer graphene. Water at the interface is defined as the adjacent water layer near graphene with a thickness of 0.5 nm, and water in the bulk corresponds to the rest region of water away from graphene.

Therefore, more overlaps are observed with the increasing layer number, indicating a better vibrational coupling at the interface. This result is consistent with the lower interfacial thermal resistance as plotted in Fig. 2. It is found that water VDOS at the interface is almost the same as that in the bulk, which is in accordance with the fact that thermal resistance is irrelevant to the size of the water layer (see supplementary material for details). In contrast, graphene VDOS in the bulk has more high-frequency modes and fewer low-frequency modes, which differs from that at the interface because the phonons in the bulk cannot couple with water directly. This difference indicates that high-frequency vibrations might have to transform into low-frequency vibrations from the bulk to the interface through interlayer scattering tunnels.

Since interlayer coupling can shift the phonon modes from high frequencies to low frequencies, we can mediate the interfacial thermal resistance by changing interlayer coupling strength. Take two-layer graphene as an example, oxygen atoms are adopted to covalently connect the graphene layers in Fig. 1(c). The interlayer atoms are randomly distributed, and the oxygen ratio is defined as $f = N_O/N_C$, where N_O is the number of oxygen atoms and N_C is the number of carbon atoms in each layer. The result of every ratio is generated from an average of five independent simulations with different random distributions of interlayer atoms. Figure 4 shows the relative thermal resistance $R_{\text{modified}}/R_{\text{unmodified}}$ with respect to the interlayer oxygen ratio. There is a peak reduction of nearly 50% corresponding to $f = 0.5\%$. It should be noted that adding interlayer atoms may impair the thermal transport at the graphene-water interface if $f \geq 1.0\%$. This abnormal dependence might be related to two competing mechanisms. On the one hand, oxygen atoms have a large atomic mass and tend to vibrate at low frequencies, and so, more low frequencies might be introduced in graphene due to C-O interactions and thus improve the thermal transport. On the other hand, interlayer coupling is suppressed as graphene layers are more connected by oxygen atoms, and hence, the heat transfer at the interface is impeded due to the reduction of out-of-plane low frequencies in graphene. Liu *et al.*[22] studied the thermal transport across graphene and silicene and also noticed that the

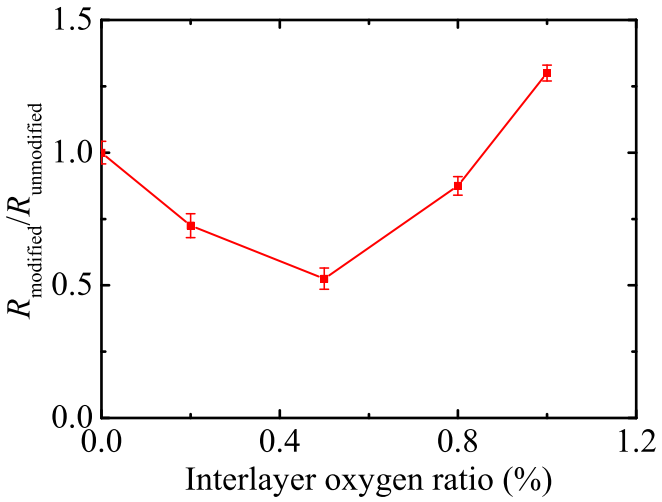

FIG. 4. Dependence of the relative interfacial thermal resistance on the ratio of interlayer oxygen atoms.

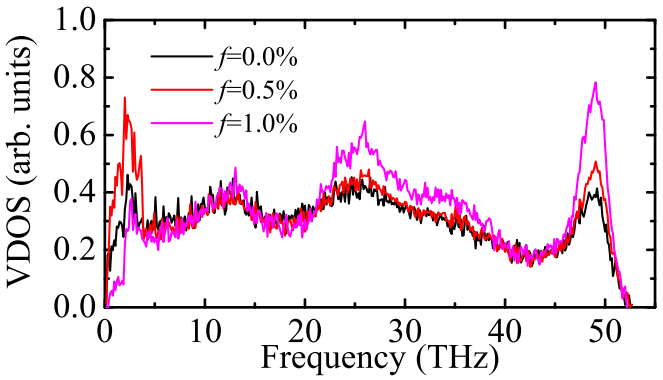

FIG. 5. Variation of the graphene vibrational density of states with respect to the ratio of interlayer oxygen atoms.

unusual dependence of interfacial thermal resistance on the hydrogenation ratio might be attributed to two competing mechanisms. To ascertain the underlying mechanisms for the non-monotonic dependence of thermal resistance on f, the VDOS is computed for different ratios in Fig. 5. It is found that more low-frequency modes (0–4 THz) are excited with $f = 0.5\%$ as compared to unmodified graphene, resulting in more VDOS overlaps with water. As to $f = 1.0\%$, few modes exist in the low-frequency region with a large population of high-frequency modes in the range of 22–40 THz and 46–50 THz, leading to a shrinkage of the VDOS overlap area. It is well understood that chemical functionalization at the interface is an efficient way to strengthen the heat transfer across SLG and the matrix.[18–20,41] Furthermore, it should be noted that interlayer coupling is of great importance with respect to the thermal transport across MLG and the matrix, and interlayer functionalization might be an additional approach to reduce the interfacial thermal resistance. The results could be useful for the experimental endeavors in preparing graphene-based composites with high thermal conductivity values. Specifically for nanofluids containing MLG, interlayer functionalization could be applied for further thermal conductivity enhancements in addition to modifying the graphene surface or increasing the temperature.[15]

In summary, the thermal transport across graphene and water is investigated via MD simulations. It is found that the interfacial thermal resistance decreases with the layer number owing to more VDOS overlaps at the interface. The thermal resistance at the graphene-water interface is tuned by introducing interlayer oxygen atoms, and a maximum reduction of ~50% is observed when the oxygen ratio is 0.5%. The unusual dependence on the oxygen ratio is related to two competing mechanisms confirmed by VDOS analyses. Our findings indicate that chemical functionalization by interlayer oxygen atoms is promising for enhancing the thermal transport across MLG and the matrix in graphene-based composites.

See supplementary material for more details about the temperature relaxation curves of graphene and water and the effects of the domain size, water thickness, and initial temperature difference on the calculated thermal resistance.

This work was financially supported by the National Natural Science Foundation of China (Grant Nos. 51676108

and 51628602), Tsinghua National Laboratory for Information Science and Technology, and the Science Fund for Creative Research Group (No. 51621062).

[1]A. A. Balandin, S. Ghosh, W. Bao, I. Calizo, D. Teweldebrhan, F. Miao, and C. N. Lau, Nano Lett. **8**(3), 902–907 (2008).
[2]S. Ghosh, I. Calizo, D. Teweldebrhan, E. P. Pokatilov, D. L. Nika, A. A. Balandin, W. Bao, F. Miao, and C. N. Lau, Appl. Phys. Lett. **92**(15), 151911 (2008).
[3]A. A. Balandin, Nat. Mater. **10**(8), 569–581 (2011).
[4]L. Lindsay, D. A. Broido, and N. Mingo, Phys. Rev. B **82**(11), 115427 (2010).
[5]D. L. Nika, A. S. Askerov, and A. A. Balandin, Nano Lett. **12**(6), 3238–3244 (2012).
[6]B.-Y. Cao, W.-J. Yao, and Z.-Q. Ye, Carbon **96**, 711–719 (2016).
[7]Z.-Q. Ye, B.-Y. Cao, W.-J. Yao, T. Feng, and X. Ruan, Carbon **93**, 915–923 (2015).
[8]J.-H. Zou and B.-Y. Cao, Appl. Phys. Lett. **110**(10), 103106 (2017).
[9]E. Pop, V. Varshney, and A. K. Roy, MRS Bull. **37**(12), 1273–1281 (2012).
[10]J. R. Potts, D. R. Dreyer, C. W. Bielawski, and R. S. Ruoff, Polymer **52**(1), 5–25 (2011).
[11]L. M. Veca, M. J. Meziani, W. Wang, X. Wang, F. Lu, P. Zhang, Y. Lin, R. Fee, J. W. Connell, and Y.-P. Sun, Adv. Mater. **21**(20), 2088–2092 (2009).
[12]K. M. Shahil and A. A. Balandin, Nano Lett. **12**(2), 861–867 (2012).
[13]A. K. Rasheed, M. Khalid, W. Rashmi, T. C. S. M. Gupta, and A. Chan, Renewable Sustainable Energy Rev. **63**, 346–362 (2016).
[14]T. T. Baby and S. Ramaprabhu, J. Appl. Phys. **108**(12), 124308 (2010).
[15]S. S. Gupta, V. M. Siva, S. Krishnan, T. S. Sreeprasad, P. K. Singh, T. Pradeep, and S. K. Das, J. Appl. Phys. **110**(8), 084302 (2011).
[16]W. Yu, H. Xie, X. Wang, and X. Wang, Phys. Lett. A **375**(10), 1323–1328 (2011).
[17]N. Shenogina, R. Godawat, P. Keblinski, and S. Garde, Phys. Rev. Lett. **102**(15), 156101 (2009).
[18]D. Konatham and A. Striolo, Appl. Phys. Lett. **95**(16), 163105 (2009).
[19]X. Shen, Z. Wang, Y. Wu, X. Liu, and J.-K. Kim, Carbon **108**, 412–422 (2016).
[20]Y. Wang, C. Yang, Y.-W. Mai, and Y. Zhang, Carbon **102**, 311–318 (2016).
[21]S. Shenogin, A. Bodapati, L. Xue, R. Ozisik, and P. Keblinski, Appl. Phys. Lett. **85**(12), 2229–2231 (2004).
[22]B. Liu, J. A. Baimova, C. D. Reddy, A. W. Law, S. V. Dmitriev, H. Wu, and K. Zhou, ACS Appl. Mater. Interfaces **6**(20), 18180–18188 (2014).
[23]M. D. Losego, M. E. Grady, N. R. Sottos, D. G. Cahill, and P. V. Braun, Nat. Mater. **11**(6), 502–506 (2012).
[24]S. Lin and M. Buehler, J. Nanotechnol. **24**(16), 165702 (2013).
[25]Z. Q. Ye and B. Y. Cao, Phys. Chem. Chem. Phys. **18**(48), 32952–32961 (2016).
[26]D. Alexeev, J. Chen, J. H. Walther, K. P. Giapis, P. Angelikopoulos, and P. Koumoutsakos, Nano Lett. **15**(9), 5744–5749 (2015).
[27]S. Plimpton, J. Comput. Phys. **117**(1), 1–19 (1995).
[28]J. Tersoff, Phys. Rev. B **37**(12), 6991 (1988).
[29]L. Lindsay and D. A. Broido, Phys. Rev. B **81**(20), 205441 (2010).
[30]J. H. Zou, Z. Q. Ye, and B. Y. Cao, J. Chem. Phys. **145**(13), 134705 (2016).
[31]H. Berendsen, J. Grigera, and T. Straatsma, J. Phys. Chem. **91**(24), 6269–6271 (1987).
[32]T. Werder, J. H. Walther, R. Jaffe, T. Halicioglu, and P. Koumoutsakos, J. Phys. Chem. B **107**(6), 1345–1352 (2003).
[33]L. Girifalco, M. Hodak, and R. S. Lee, Phys. Rev. B **62**(19), 13104 (2000).
[34]S. T. Huxtable, D. G. Cahill, S. Shenogin, L. Xue, R. Ozisik, P. Barone, M. Usrey, M. S. Strano, G. Siddons, M. Shim, and P. Keblinski, Nat. Mater. **2**(11), 731–734 (2003).
[35]J. W. Pomeroy, R. B. Simon, H. Sun, D. Francis, F. Faili, D. J. Twitchen, and M. Kuball, IEEE Electron Device Lett. **35**(10), 1007–1009 (2014).
[36]W. G. Hoover, Phys. Rev. A **31**(3), 1695 (1985).
[37]A. Stukowski, Model. Simul. Mater. Sci. Eng. **18**(1), 015012 (2010).
[38]L. Hu, T. Desai, and P. Keblinski, Phys. Rev. B **83**(19), 195423 (2011).
[39]J. Chen, G. Zhang, and B. Li, Appl. Phys. Lett. **95**(7), 073117 (2009).
[40]B. Li, L. Wang, and G. Casati, Phys. Rev. Lett. **93**(18), 184301 (2004).
[41]T.-Y. Wang and J.-L. Tsai, Comput. Mater. Sci. **122**, 272–280 (2016).